Search for compressed mass Higgsino production with soft lepton tracks with the CMS experiment in proton-proton collision data at $\sqrt{s} = 13$ TeV

vorgelegt von

Yuval Nissan

im August 2022

Universität Hamburg

DER FORSCHUNG | DER LEHRE | DER BILDUNG

Abstract This is the abstract

Contents

7 Jet Isolation and Non-Isolated Background Estimation   **27**

8 Summary   **29**

9 Latex stuff   **31**

Glossary   **35**

Acronyms   **37**

Chapter 1

Introduction

This is a line in introduction. This is the introduction to the thesis.

Chapter 2

Quantum Field Theory and The Standard Model

2.1 Quantum Field Theory

2.2 The Standard Model of particle physics

2.2.1 The particle content

Chapter 3

Supersymmetry

3.0.1 Phenomenology of Higgsino production

Chapter 4

Multivariate Statistics

4.1   Decision Trees

Chapter 5

Experimental setup: Collider, detector, and algorithms

Chapter 6

Search for compressed Higgsinos with soft lepton tracks

6.1   Motivation

6.2   Previous searches

6.3   Signal models

The signal models considered in this analysis are based on **FiXme Note: fill in signal model stuff**.
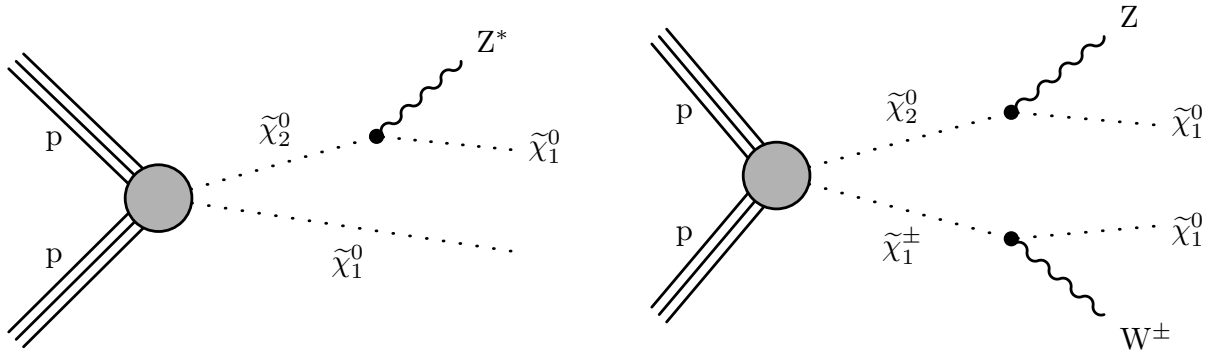
Figure 6.1: Production and decay of electroweakinos in the higgsino simplified model through $\widetilde{\chi}_2^0\,\widetilde{\chi}_1^0$ (left) and $\widetilde{\chi}_2^0\,\widetilde{\chi}_1^\pm$ (right).

6.4   Signal signature and base selection

To build an effective analysis strategy, the signal kinematics must be studied and exploited. The electroweakino production in question exhibit unique features which can be used in order to discriminate between the signal and the Standard Model (SM) background. It is important to explore these signal distributions in order to define a preselection, or a base cut, that will serve the purpose of retaining as much signal as possible while rejecting as much background. All of the following distributions were plotted by weighting the simulation to Run II luminosity of $\mathcal{L} = 135\,\mathrm{fb}^{-1}$ and requiring at least one jet in the event with $p_{\mathrm{T}} \geq 30\,\mathrm{GeV}$ and $|\eta| < 2.4$. Further selection might apply and will be listed in each section in that case.

6.4.1 Missing Transverse Energy

One property that essentially all Dark Matter (DM) searches have in common is the presence of a DM candidate in the production. The exact identity and properties of said particle (or particles in the case multiple DM candidates) vary, but they do share a lot in common. The DM candidate in our Supersymmetry (SUSY) search is the neutralino, which is a type of DM candidate referred to as a Weakly Interacting Massive Particle (WIMP). A WIMP, broadly speaking, is a new elementary particle which interacts via gravity and any other force (or forces), potentially not part of the SM itself, which is as weak as or weaker than the weak nuclear force, but also non-vanishing in its strength. That essentially means that such candidate is neutral, and therefore not interacting via the electromagnetic force. A neutral particle that interacts neither electromagnetically nor via the strong force (i.e. colorless) will escape detection and will leave traces in the form of a transverse momentum imbalance, which we refer to as $E_{\mathrm{T}}^{\mathrm{miss}}$ (Missing Transverse Energy or Missing Transverse Momentum). Our signal contains two DM candidates in the production, which are the Lightest SUSY Particles (LSPs), the neutralinos $\widetilde{\chi}_1^0$. We therefore expect the signal to contain considerable magnitude of $E_{\mathrm{T}}^{\mathrm{miss}}$. As described in 6.7.3, **FiXme Note: make sure we described both met and mht** we are more interesting in $H_{\mathrm{T}}^{\mathrm{miss}}$, which is highly correlated with $E_{\mathrm{T}}^{\mathrm{miss}}$, due to our definition of lepton isolation and its use in the background estimation methods. Nonetheless, we will look at both $E_{\mathrm{T}}^{\mathrm{miss}}$ and $H_{\mathrm{T}}^{\mathrm{miss}}$ observables. **FiXme Note: make sure we define the different deltaM somewhere**
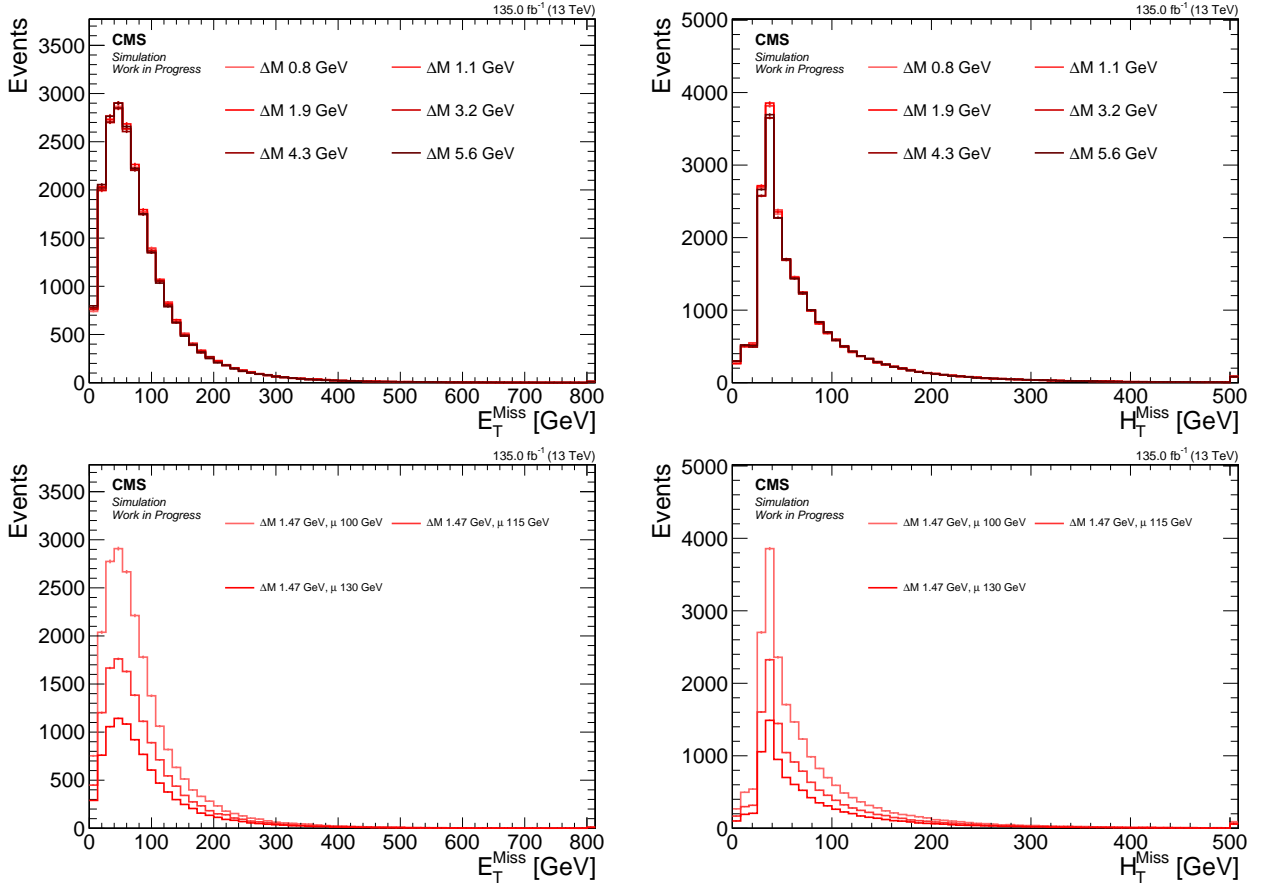
Figure 6.2: Signal distributions for $E_{\mathrm{T}}^{\mathrm{miss}}$ (left) and $H_{\mathrm{T}}^{\mathrm{miss}}$ (right) comparing various Δm with a fixed higgsino parameter $\mu = 100\,\mathrm{GeV}$ (upper), and comparing various higgsino parameters μ with fixed $\Delta \mathrm{m} = 1.47\,\mathrm{GeV}$ (lower).

As we expect, $E_{\mathrm{T}}^{\mathrm{miss}}$ and $H_{\mathrm{T}}^{\mathrm{miss}}$ are hardly affected by the different choices for Δm, while the higgsino parameter μ affect the distributions above all through its lower production cross section

for higher higgsino parameter μ. As discuss at 6.8, the region of interest lie at $H_T^{miss} \geq 220$ for triggering purposes. Even though this is quite a harsh and inefficient cut, one must look also at the SM background at the regions of $H_T^{miss} < 220$ and $H_T^{miss} \geq 220$ to conclude that most of the sensitivity comes from the $H_T^{miss} \geq 220$ region, since the production of real H_T^{miss} (or E_T^{miss}) result from the production of neutrinos in the event, and these are much less common than Quantum Chromodynamics (QCD) events which swarm the $H_T^{miss} < 220$ region. Therefore, cutting at $H_T^{miss} \geq 220$ might be inefficient, but results in high sensitivity.

6.4.2 Jets and hardronic activity

Since the neutralinos $\widetilde{\chi}_1^0$ escaping the detector are the contributors to the H_T^{miss} and in doing so the drivers of the sensitivity in high H_T^{miss} region, we want them to be as boosted as possible, i.e., with the highest transverse momentum p_T as possible. A widely used approach is to require **FiXme Note: add citation** an Initial State Radiation (ISR) jet in the event. An ISR jet is formed when one of the incoming protons emit radiation (such as a photon or a gluon) before the interaction **FiXme Note: add citation and maybe reference to other section**. If a jet with high enough p_T is emitted, the rest of the interaction is recoiled against this jet and boosting it in the other direction. This way, the boosted neutralinos $\widetilde{\chi}_1^0$ will result in higher H_T^{miss}. As described in **FiXme Note: ref**, we require the jets to have $p_T \geq 30\,\text{GeV}$ and be located within the tracker acceptance ($|\eta| < 2.4$). We require at least one such jet in the event.
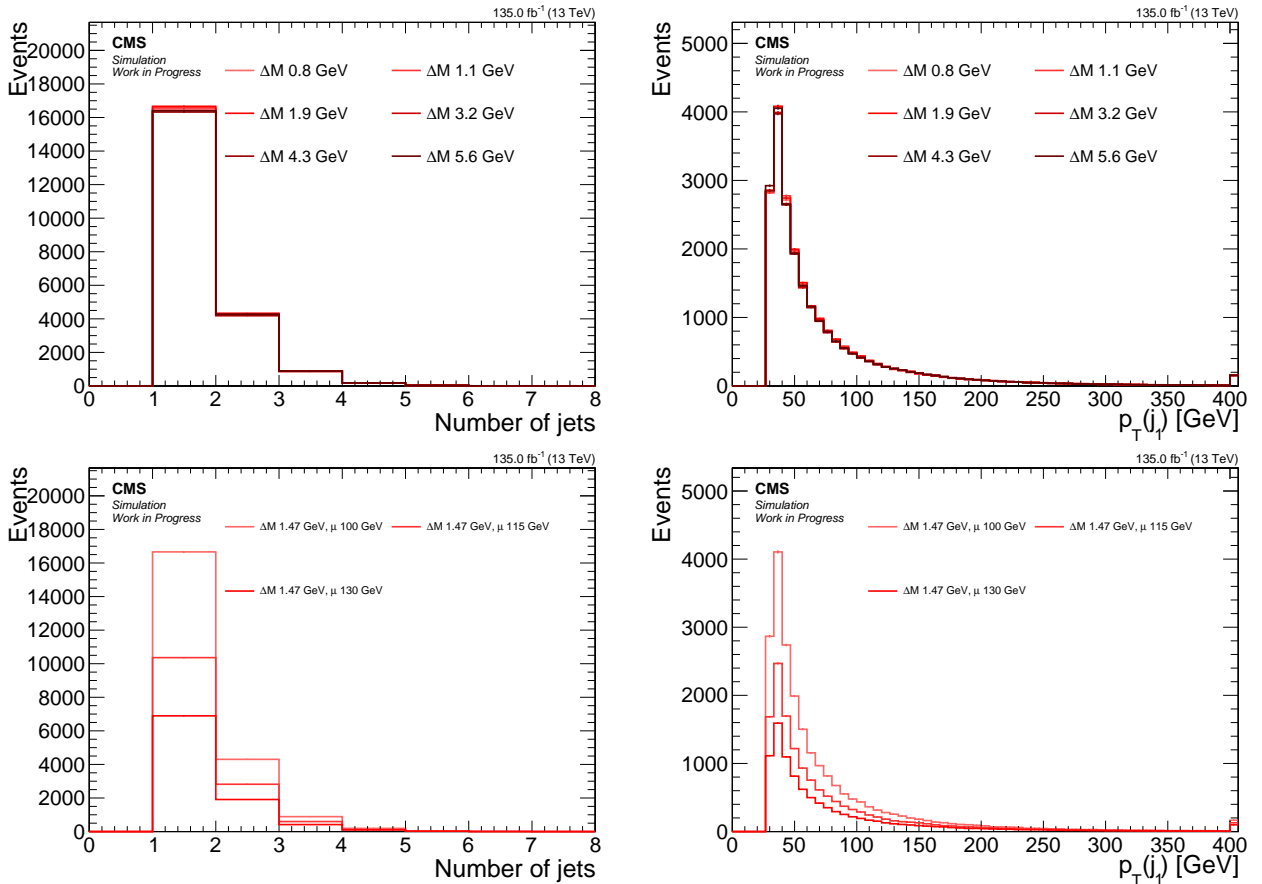

Figure 6.3: Signal distributions for *number of jets* (left) and *leading jet* p_T (right) comparing various Δm with a fixed higgsino parameter $\mu = 100\,\text{GeV}$ (upper), and comparing various higgsino parameters μ with fixed $\Delta m = 1.47\,\text{GeV}$ (lower).

Our signal signature does not include a b-jet, i.e., a jet resulting from a bottom quark hadronization (either resulting from a top quark or not). We therefore seek to exploit this knowledge by vetoing b-tagged jets in the event. As described in **FiXme Note: add ref** we are using DEEPCSV flavor tagging discriminant with a medium working point. As can be seen in these distributions, most of the signal lie in the 0 bin, and we will therefore veto any b-tagged jet, which retains most of the signal, but rejects a lot of SM background, such as arising from $t\bar{t}$ events.
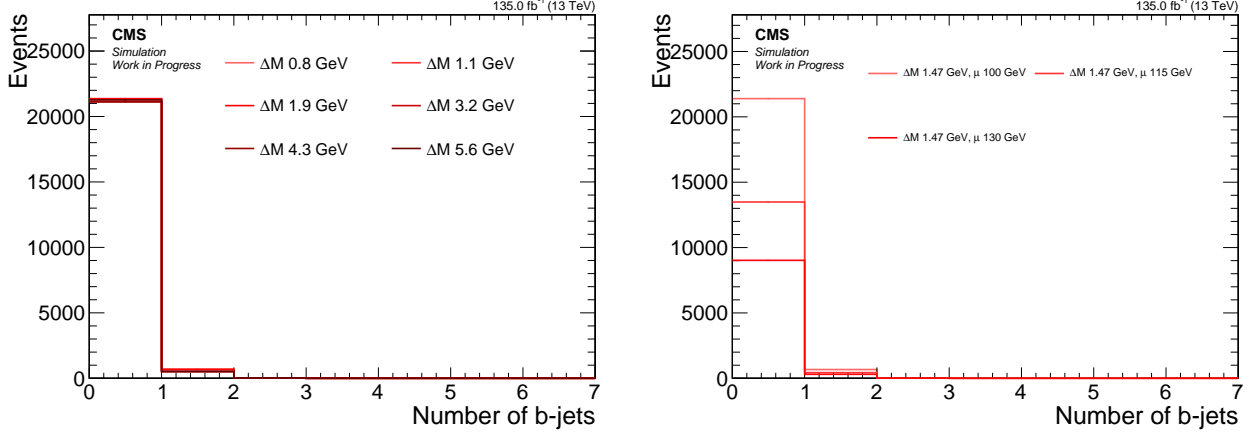

Figure 6.4: Signal distributions for *number of b-tagged jets* comparing various Δm with a fixed higgsino parameter $\mu = 100$ GeV (left), and comparing various higgsino parameters μ with fixed Δm $= 1.47$ GeV (right).

Since we are requiring an ISR jet in the event, we expect the E_T^{miss} and the H_T^{miss} to point in the opposite direction of the jet, or at least in an angel close to π. Events with multiple jets in the SM background such as arising from QCD will not exhibit such a feature. In order to reduce QCD background, we require $\min \Delta\phi\left(H_T^{miss}, \text{jets}\right) > 0.4$.

6.4.3 Base selection

We recap the section by summarizing the base selection of our analysis. This base selection, or preselection as we might use call it interchangeably, is applied to all analysis categories.

Table 6.1: Base selection applied to all analysis categories

Variable	Value
H_T^{miss} [GeV]	≥ 220
$N_{\text{jets}}\left(p_T \geq 30\,\text{GeV and } |\eta| < 2.4\right)$	≥ 1
$N_{\text{b-jets}}\left(p_T \geq 30\,\text{GeV and } |\eta| < 2.4\right)$	0
$\min \Delta\phi\left(H_T^{miss}, \text{jets}\right)$	> 0.4

6.4.4 Dilepton kinematics

Thus far we have looked at kinematic distributions ignoring the leptons in event. However, the most distinct features of the signal lie in the dilepton system. To fully understand the unique phase space of the dilepton system, we first look at generator level distributions and then look at what effects does reconstruction have on those observables. In addition, since the most sensitive category is the dimuon category due to its much lower threshold on the
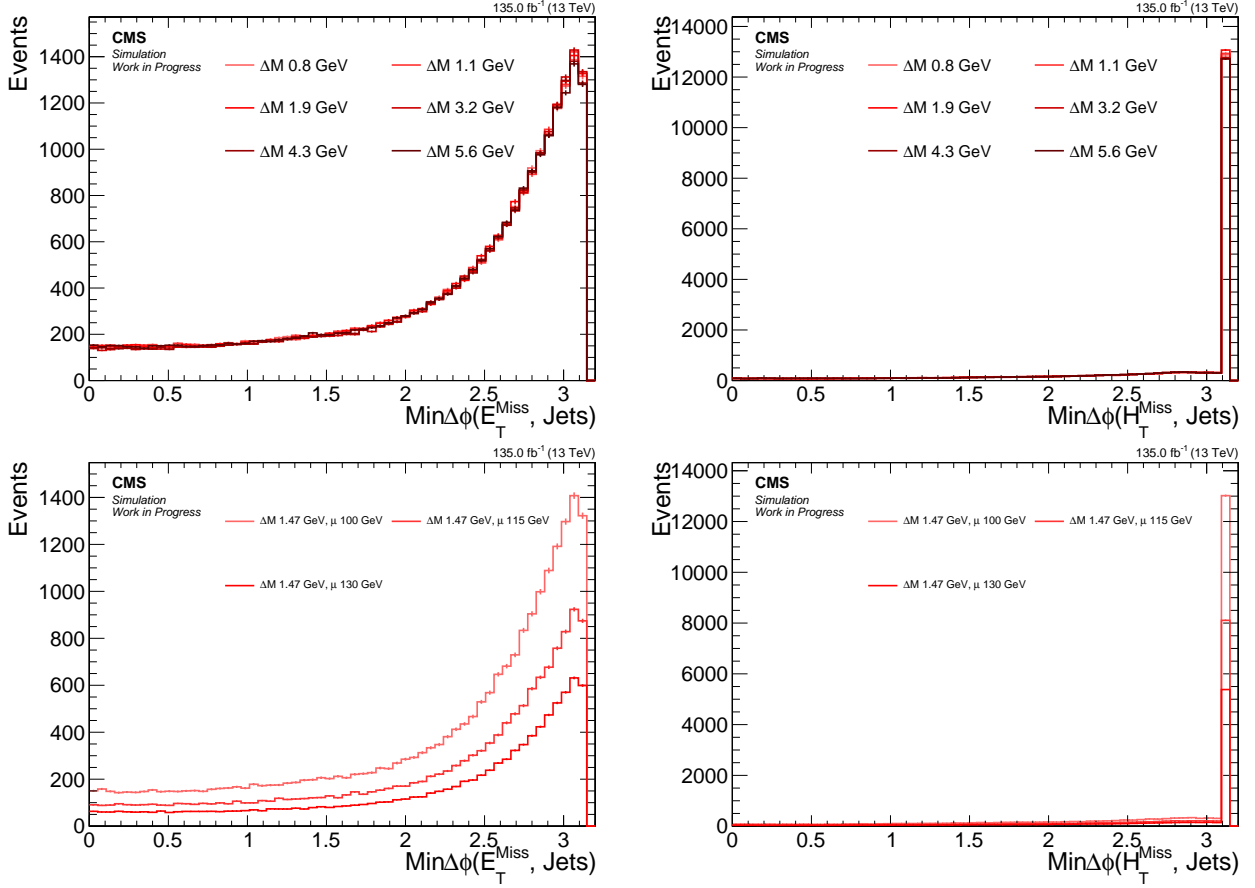
Figure 6.5: Signal distributions for $\min \Delta\phi \left(E_{\mathrm{T}}^{\mathrm{miss}}, \mathrm{jets} \right)$ (left) and $\min \Delta\phi \left(H_{\mathrm{T}}^{\mathrm{miss}}, \mathrm{jets} \right)$ (right) comparing various Δm with a fixed higgsino parameter $\mu = 100\,\mathrm{GeV}$ (upper), and comparing various higgsino parameters μ with fixed $\Delta m = 1.47\,\mathrm{GeV}$ (lower).

transverse momentum, these events are shown in the following sections, leaving the events with two electrons to the appendix **FiXme Note: ref**.

Since the kinematics changes dramatically as a function of Δm, but changes almost only in overall normalization due to the production cross section as a function of the higgsino parameter μ, in the following sections, we set the higgsino parameter to $\mu = 100\,\mathrm{GeV}$ and vary the Δm.

Muon η and transverse momentum p_{T}

The transverse momentum p_{T} distribution of the muons and our access to a subset of its full range, have dramatic effect on the signal acceptance and the sensitivity. The muon reconstruction process and details are discussed in **FiXme Note: ref**. The selection we apply to the muons in this analysis is described in 6.7.2 and will be referred to here as *analysis selection*. In this section we would like to consider specifically the importance of the p_{T} on the signal and its dilepton kinematic distributions.

We begin by having a look at the generator level distribution of p_{T}, or in other words, the so-called *truth* distributions, which do not exhibit any detector or reconstruction features, and compare to the reconstructed distribution.

By comparing the generator level to the reconstruction level of the inclusive p_{T} distribution, we see that a reshaping occurs at around $3\,\mathrm{GeV}$. A significant portion of the generated muons with $p_{\mathrm{T}} < 3\,\mathrm{GeV}$ are being lost in reconstruction. The reconstructed subleading p_{T} distribution has a camel shape whereby the efficiency drops bellow p_{T} of $3\,\mathrm{GeV}$ and only partially regained at $p_{\mathrm{T}} < 3\,\mathrm{GeV}$. This is a detector effect and can be seen more clearly when we split the p_{T}
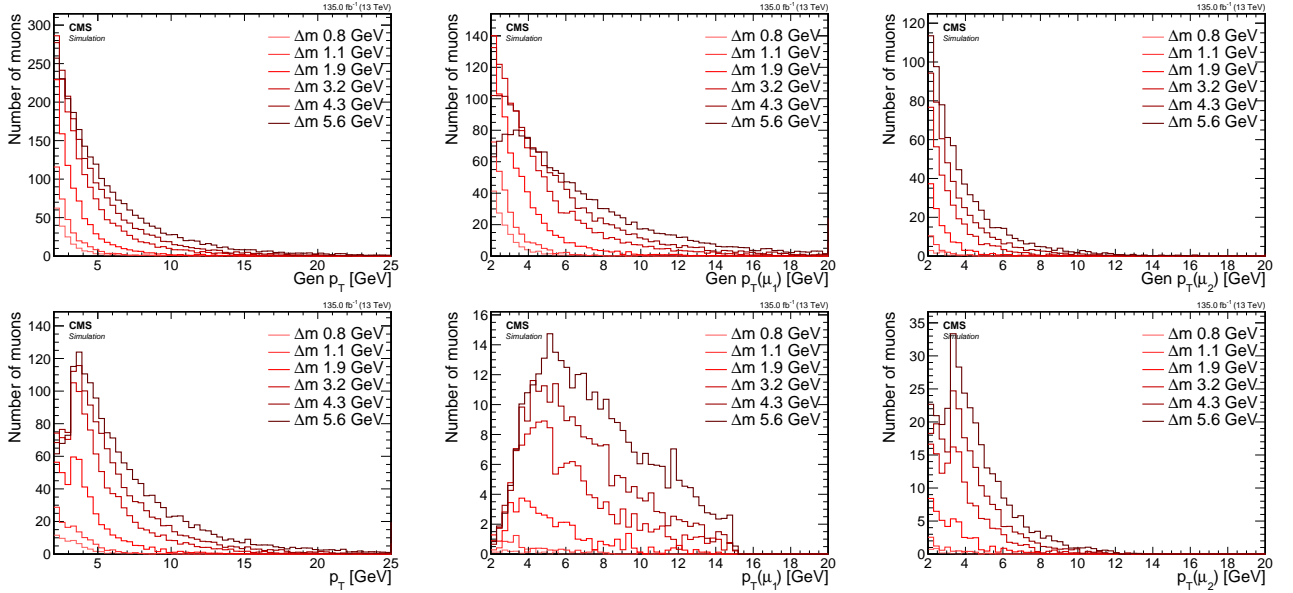
Figure 6.6:   Signal p_T distributions for inclusive (left), leading muon μ_1 (middle), subleading muon μ_2 (right) at generator level (top) and reconstruction level passing analysis selection (bottom).

distribution into a barrel ($|\eta| < 1.2$) and encaps ($|\eta| \geq 1.2$) portions.

The picture becomes much clearer in regards to the reconstruction efficiency as a function of p_T. When comparing the generator level distribution of the barrel muons on the top left with its constructed counterpart on the bottom left, we see that the barrel is almost completely unable to reconstruct muons with $p_\mathrm{T} < 3\,\mathrm{GeV}$, while the endcaps, shown on the left, are able to do so. As we will see in the $m_{\ell\ell}$ and ΔR upcoming sections (6.4.4 and 6.4.4), since those distribution have an important relationship, that has consequences in regards to reshaping kinematic distributions, as well as signal acceptance in general. Since the low region of $2 \leq p_\mathrm{T} \leq 3.5\,\mathrm{GeV}$ is crucial in giving us access to low Δm signal points, it is achieved, as can be seen here, mainly with the help of the muon chamber endcaps.

Since the barrel and endcaps are seperated by different regions of η, $|\eta| < 1.2$ for barrel and $|\eta| \geq 1.2$ for endcaps, it worth taking a look at the η distributions of the muons as well.

Our muons analysis selection picks only muons in the tracker range of $|\eta| < 2.4$ which is the reason why the reconstruction plots on the bottom do not have muons with $|eta| > 2.4$. We see that the main effect going from the inclusive $|\eta|$ in generator level to the reconstructed counter part, is the flattening of the distribution due to the loss of muons with $|eta| < 1.2$ in the barrel for muons with $p_\mathrm{T} < 3\,\mathrm{GeV}$.

With the understanding of the reconstruction effects on the p_T and η distributions of the muons, we are equipped to look further into other kinematic variables of the dilepton system.

Invariant mass $m_{\ell\ell}$

The invariant mass of the two leptons that result from the decay of the $\widetilde{\chi}_2^0$ has a unique shape due to the limited allowed phase space of the leptons as part of the 3-body decay. Since the $\widetilde{\chi}_2^0$ decays into $\widetilde{\chi}_1^0$ and $\ell^+\ell^-$ through a Z^*, the allowed phase space of the dilepton pair is restricted to the mass difference between $\widetilde{\chi}_2^0$ and $\widetilde{\chi}_1^0$, i.e., Δm. We therefore expect the $m_{\ell\ell}$ distribution to have an edge at Δm.

We see the original invariant mass of the muons $m_{\mu\mu}$ on the left. For each signal point, the edge of the $m_{\mu\mu}$ distribution is right at the corresponding Δm. However, once we cut on the muons p_T and require $p_\mathrm{T} \geq 2\,\mathrm{GeV}$, the shape shifts, and the efficiency in the lower Δm drops
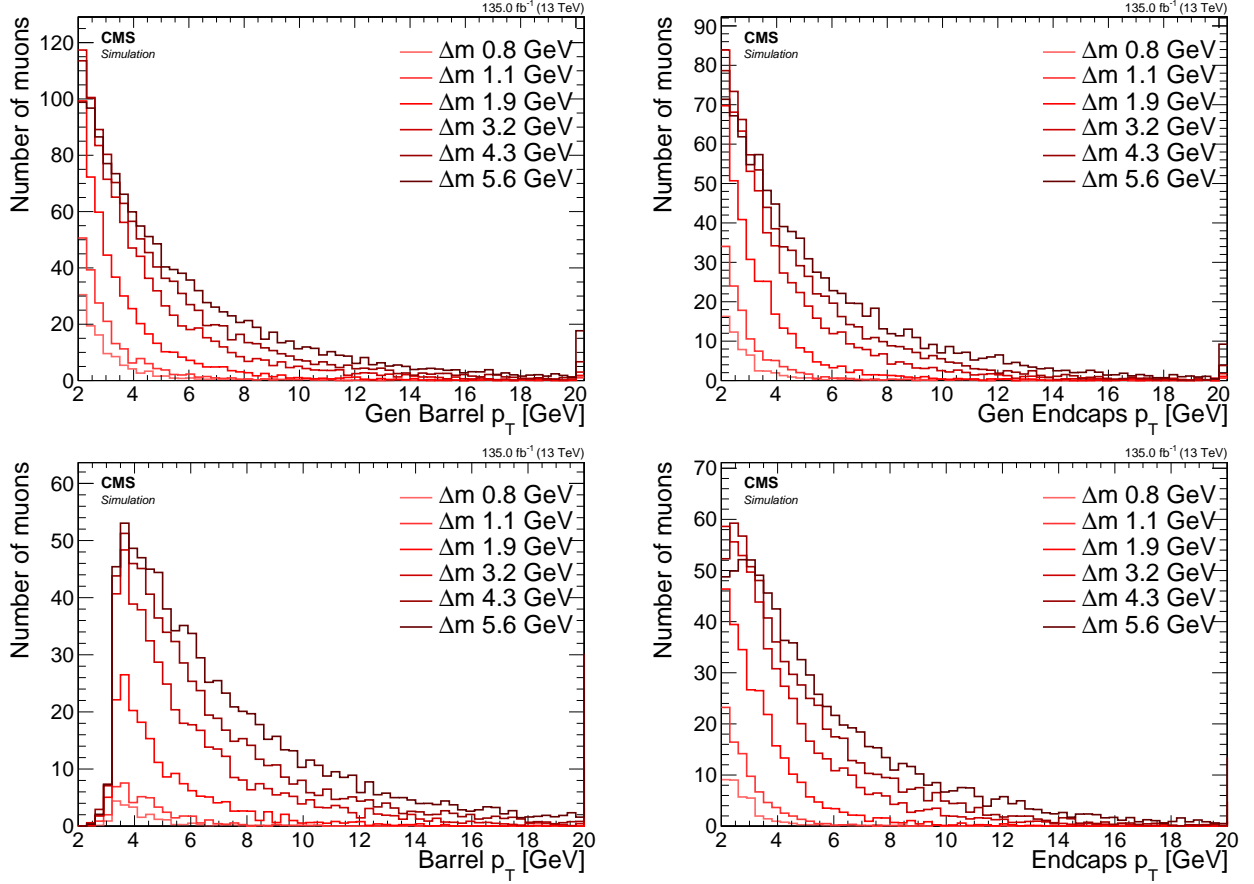
Figure 6.7: Signal inclusive p_T distributions for barrel $|\eta| < 1.2$ (left) and endcaps $|\eta| \geq 1.2$ (right) at generator level (top) and reconstruction level passing analysis selection (bottom).

dramatically, as can be seen from the middle plot. Lastly, the effect of orthogonalizing phase space to the SOS analysis can be seen on the right most plot. The effect is strongest in high Δm and quite subtle in low Δm.

To understand the reshaping that happens to the $m_{\mu\mu}$ shape, we look at the relationship between the p_T of the muons (leading muon denoted μ_1 while subleading muon is denoted μ_2) and the invariant mass one a signal with low Δm of $1.13\,\text{GeV}$ and one with high Δm of $5.63\,\text{GeV}$.

We have established earlier that the invariant mass distribution has an edge at the Δm and one can read the value of Δm from these plots. Another interesting feature to notice in these plots is that there is also a lower edge in the Δm distribution at around $\sim 0.2\,\text{GeV}$ and that is of course due to each muon having a mass of around $\sim 0.1\,\text{GeV}$. We can clearly see now that by cutting on both muons at $p_T \geq 2\,\text{GeV}$, we are loosing a lot of the signal. This effect, in fact, becomes quite substantial for the low $\Delta m = 1.13\,\text{GeV}$ (top row). We quantify this effect by making a cutflow table where each row represents a cut, and its efficiency is calculated by dividing the number of events passing the cut by the number of events in the line before it. The first line is our baseline of all dimuon events with at least one jet with $p_T \geq 30\,\text{GeV}$ and $|\eta| < 2.4$ and has an efficiency of 1 by definition. The event number is weighted to Run II luminosity of $\mathcal{L} = 135\,\text{fb}^{-1}$.

We observe that for the low Δm of $1.13\,\text{GeV}$ the cut of $p_T \geq 2\,\text{GeV}$ is really hurting the acceptance of the signal with only 1.5% of signal remaining. In contrast, the orthogonality condition of requiring $p_T(\mu_2) \leq 3.5\,\text{GeV}$ or $\Delta R(\ell\ell) \leq 0.3$ is not effecting it any further. The picture is different for the high Δm of $5.63\,\text{GeV}$ where the p_T cut is cutting away more than half of the signal and the SOS orthogonality an additional two thirds.
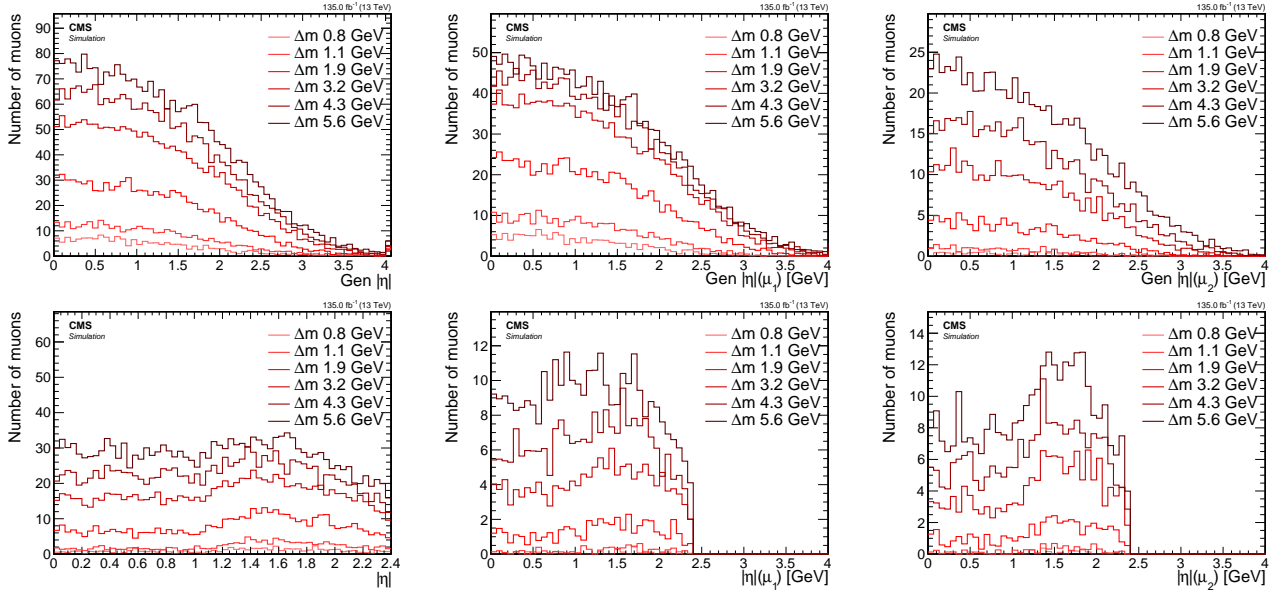
Figure 6.8: Signal $|\eta|$ distributions for inclusive (left), leading muon μ_1 (middle), subleading muon μ_2 (right) at generator level (top) and reconstruction level passing analysis selection (bottom).
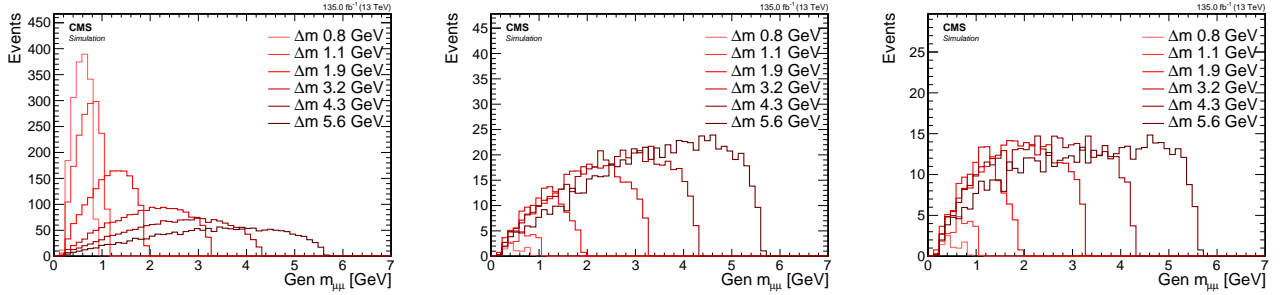

Figure 6.9: Signal generator level $m_{\ell\ell}$ distributions with no cuts (left), with $p_{\mathrm{T}}\left(\mu_i\right) > 2\,\mathrm{GeV}$, $i = 1,2$ (middle) and with SOS orthogonality condition $p_{\mathrm{T}}\left(\mu_i\right) > 2\,\mathrm{GeV}$, $p_{\mathrm{T}}\left(\mu_2\right) \leq 3.5\,\mathrm{GeV}$ or $\Delta R \leq 0.3$ (right).

Since we have just established that due to the relationship between p_{T} and $m_{\ell\ell}$, the p_{T} distribution directly effects $m_{\ell\ell}$, we should also have a look at how to reconstruction effects discussed at 6.4.4 might effect the $m_{\mu\mu}$ distribution as well.

It's interesting to compare these distributions to the two right ones in the generator level version at 6.9. We see that not only less events survive the reconstruction, but also that some Δm model points peak between $1\,\mathrm{GeV}$ to $2\,\mathrm{GeV}$ with SOS orthogonality condition applied. The reconstruction and selection efficiency is discussed in more details in **FiXme Note: ref**.

Lepton separation ΔR

The lepton separation is defined by $\Delta R = \sqrt{\left(\Delta\eta\right)^2 + \left(\Delta\phi\right)^2}$ where η is the pseudorapidity and ϕ is the azimuthal angle measured in radians. ΔR plays a major role in this analysis since the leptons tend to be produced in proximity to each other and thus to defy standard definitions of isolation. Special care is taken to ensure that the collimated nature of the leptons can still be used to distinguish the otherwise isolated leptons in the signal from the non-isolated leptons in the SM background. An additional point of interest is with respect to previous SOS analysis **FiXme Note: cite** that had a requirement of $\Delta R\left(\ell\ell\right) > 0.3$ which we attempt to revert here
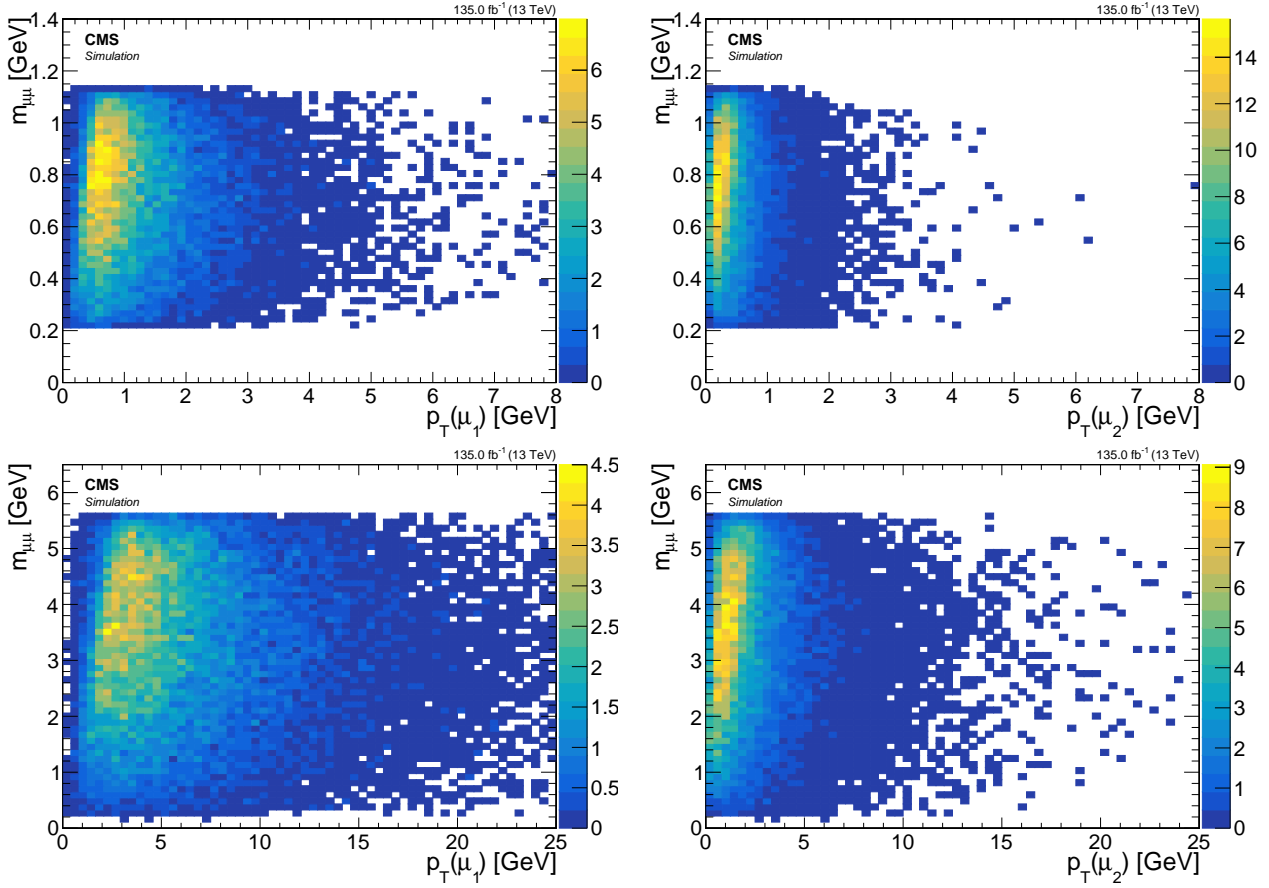
Figure 6.10: Signal $m_{\mu\mu}$ vs. p_T for leading lepton μ_1 (left) and subleading lepton μ_2 (right) for $\Delta m = 1.13\,\mathrm{GeV}$ (top) and $\Delta m = 5.63\,\mathrm{GeV}$ (bottom).

for orthogonality purposes.

In similar fashion to the invariant mass in 6.4.4, we look at distributions of ΔR for various choices of Δm with different cuts applied, and observe their effect.

As can be seen on the left plot, roughly the same amount of events are produced for all Δm model points, but when applying a cut of $p_T(\mu) > 2\,\mathrm{GeV}$, a hierarchy of Δm points forms, with less events as Δm becomes smaller (middle plot). The spike on the right plot is due to the SOS orthogonality condition which requires $\Delta R(\ell\ell) \leq 0.3$ as one of two conditions in an or statement. To understand the shaping and hierarchy formation due to the p_T cut, we repeat the trick from the $m_{\mu\mu}$ in 6.4.4 and plot the p_T of the muons vs. $\Delta R(\ell\ell)$.

Now the hierarchy can be understood by observing that for $\Delta m = 1.13\,\mathrm{GeV}$, cutting $p_T(\mu_2) \geq 2\,\mathrm{GeV}$ will limit the range of $\Delta R(\mu\mu)$ to less than 0.4 while leaving quite a large range exceeding 3 for the $\Delta m = 5.63\,\mathrm{GeV}$ model point.

We conclude therefore, that even before taking into consideration reconstruction efficiency of the leptons, to gain access and sensitivity to the low Δm model points, we must be able to probe low $\Delta R(\ell\ell)$ values, potentially with values less than 0.3. In the next sections we will need to study reconstructed leptons and define isolation criteria that will enable us to retain signal points with close lepton pairs.

As we have seen for $m_{\mu\mu}$ in 6.4.4, reconstruction has an effect on both the shape and overall count of events. We look here at those effects on the $\Delta R(\mu\mu)$ distributions.

When we compare the reconstructed $\Delta R(\mu\mu)$ distributions 6.14 to the generator level ones at 6.12 we see that the main effect of the reconstruction on the $\Delta R(\mu\mu)$ is the overall normalization due to reconstruction efficiency.
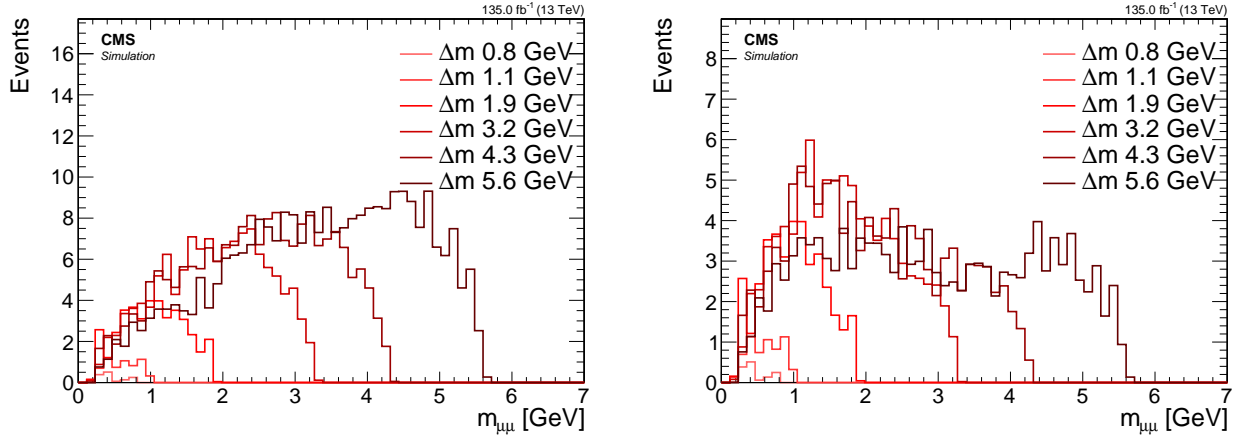
Figure 6.11:   Signal reconstructed $m_{\mu\mu}$ with basic analysis selection (left) and additional SOS orthogonality condition (right).
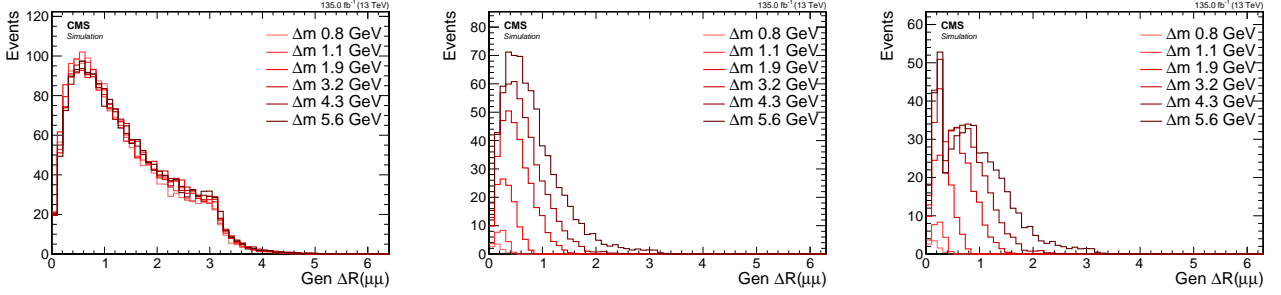

Figure 6.12:   Signal generator level ΔR distributions with no cuts (left), with $p_{\mathrm{T}}\left(\mu_i\right) > 2\,\mathrm{GeV}$, $i = 1, 2$ (middle) and with SOS orthogonality condition $p_{\mathrm{T}}\left(\mu_i\right) > 2\,\mathrm{GeV}$, $p_{\mathrm{T}}\left(\mu_2\right) \leq 3.5\,\mathrm{GeV}$ or $\Delta R \leq 0.3$ (right).

6.4.5   Main drivers of sensitivity

We attempt to draw conclusion from this signal distribution studies in regards to the main drivers to the sensitivity of different model points of this analysis, as well as of future analysis that might attempt to expend on this one. In this section we have not looked at SM background at all. Therefore, it is hard to conclude what effects changing the cuts to $E_{\mathrm{T}}^{\mathrm{miss}}$ or other event level observables might have. However, one thing is very clear from examining the dilepton kinematics and that is that to gain access to low Δm model points, one must lower the threshold on of p_{T} in the selection of the decay leptons and make sure to also be able to probe low ΔR. Another driver of the sensitivity at all Δm model points is the luminosity, since the production cross section drops as a function of the higgsino mass parameter μ.

We will explore in the next section how we are able to lower the threshold on the muons transverse momentum as well as dealing with collimated leptons that might pose a challenge.
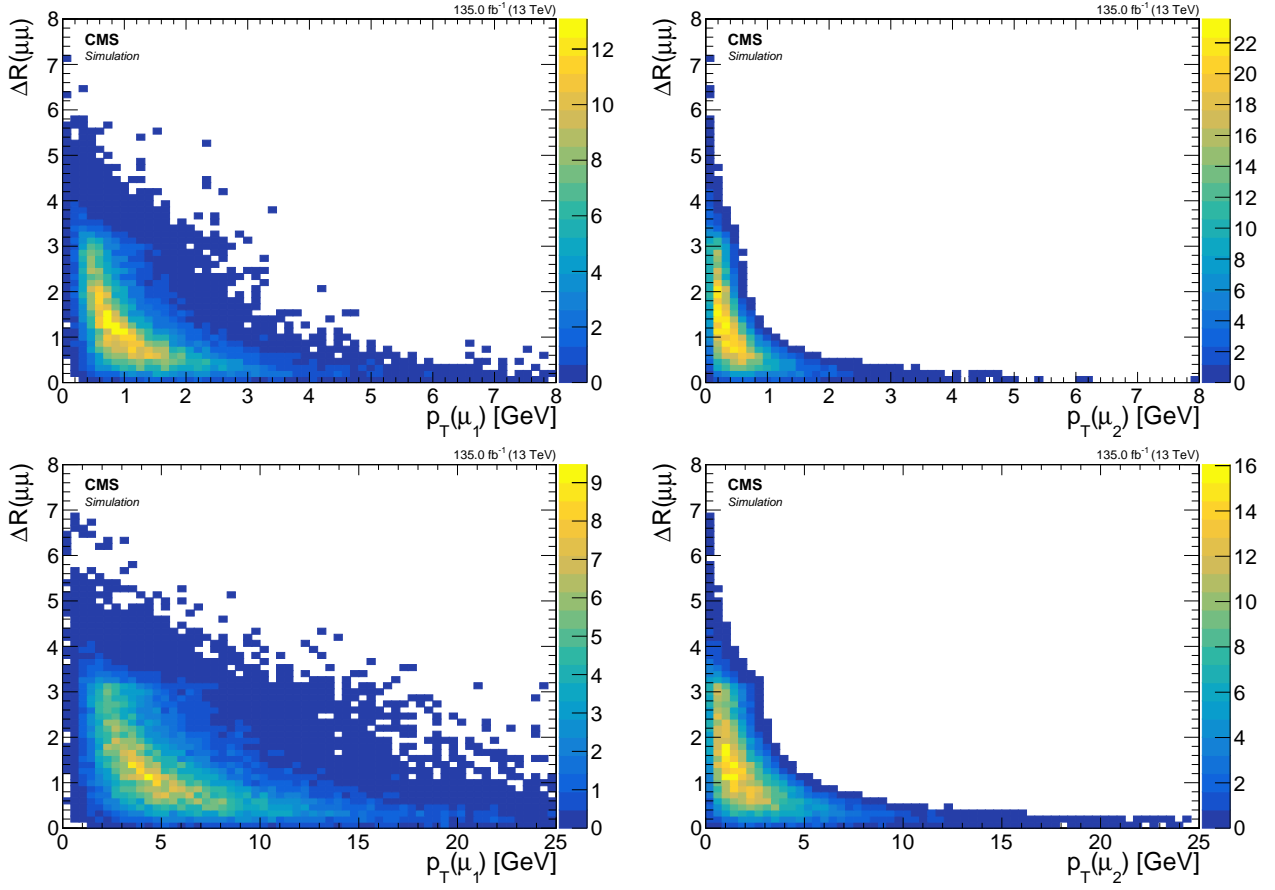
Figure 6.13: Signal $\Delta R (\mu\mu)$ *vs.* p_{T} for leading lepton μ_1 (left) and subleading lepton μ_2 (right) for $\Delta\mathrm{m} = 1.13\,\mathrm{GeV}$ (top) and $\Delta\mathrm{m} = 5.63\,\mathrm{GeV}$ (bottom).

6.5 Search strategy

6.6 Simulated samples

6.6.1 Standard Model simulated samples

6.6.2 Signal simulated samples

6.7 Object Definition and Selection

6.7.1 Electrons

Signal Electron Selection

Additional Electron Veto

6.7.2 Muons

Signal muon selection

Additional muon veto

6.7.3 Missing transverse energy
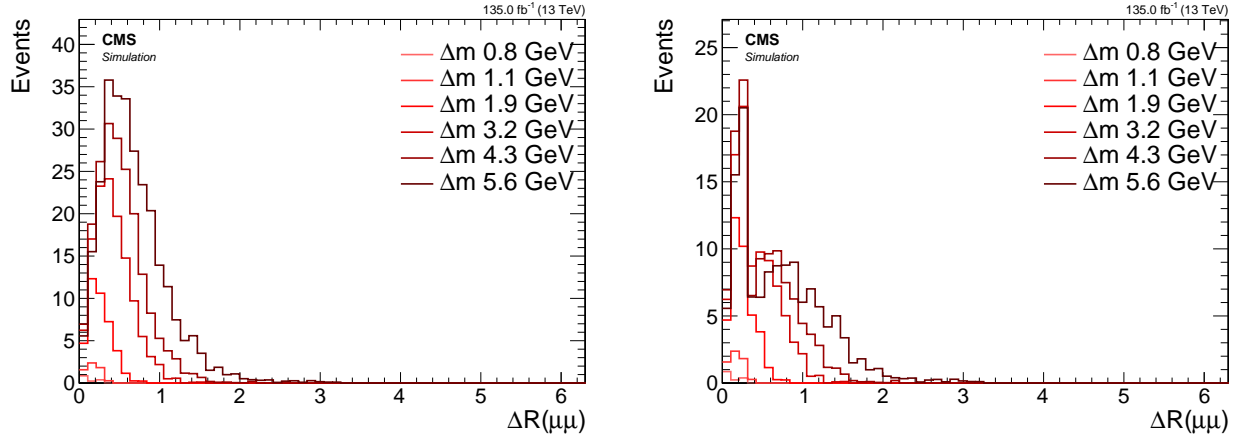
Figure 6.14: Signal reconstructed $\Delta R\,(\mu\mu)$ with basic analysis selection (left) and additional SOS orthogonality condition (right).

Table 6.2: Generator level efficiency on muons selections

Cut	Number of events		Efficiency	
	$\Delta m = 1.13\,\text{GeV}$	$\Delta m = 5.63\,\text{GeV}$	$\Delta m = 1.13\,\text{GeV}$	$\Delta m = 5.63\,\text{GeV}$
Baseline	1710.7	1743.9	1	1
$p_\text{T} \geq 2\,\text{GeV}$	24.7	724.9	0.015	0.41
SOS orthogonality	24.7	490.6	1	0.68
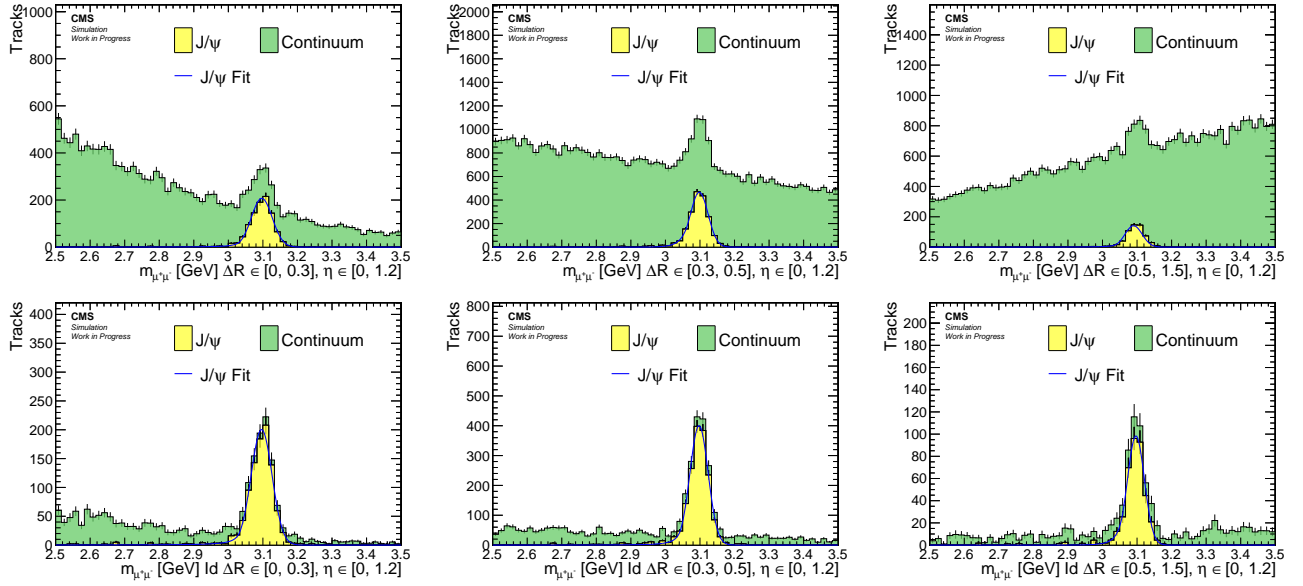
Figure 6.15: Barrel Muons BG
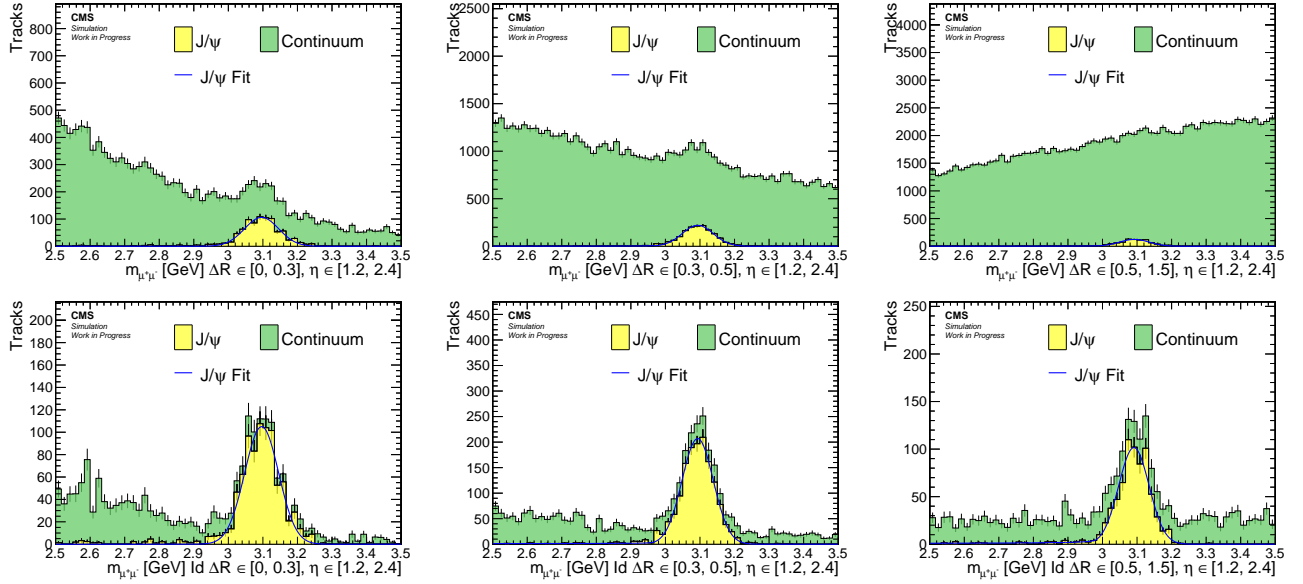
Figure 6.16: Endcaps Muons BG
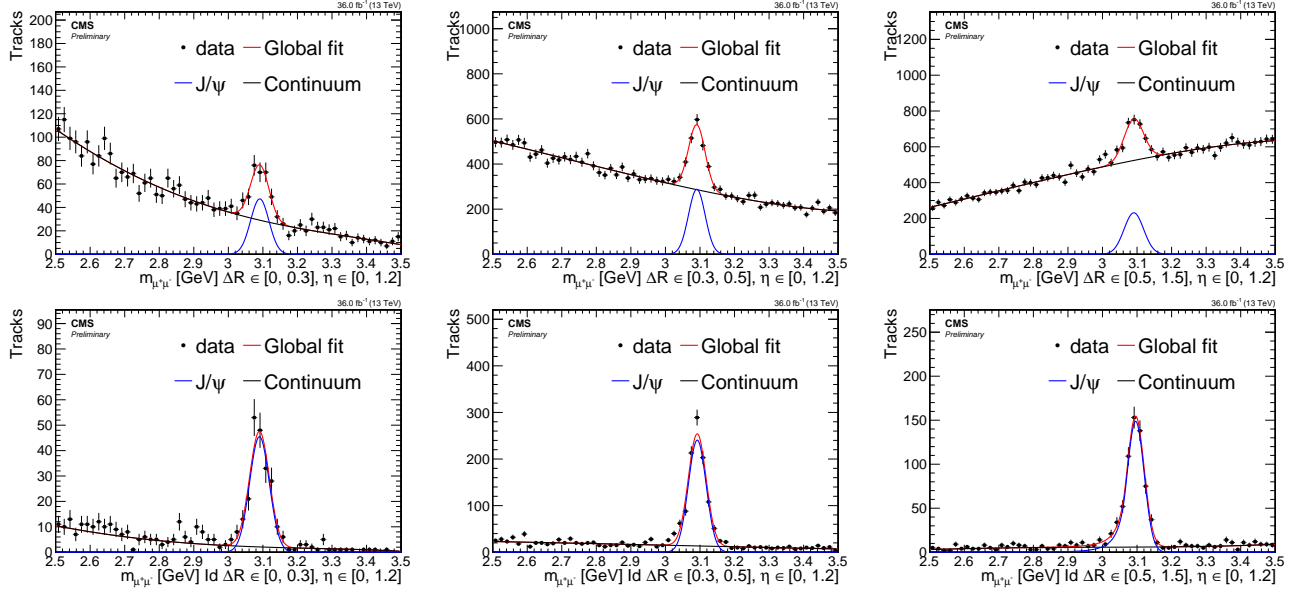
Figure 6.17: Barrel Muons Data
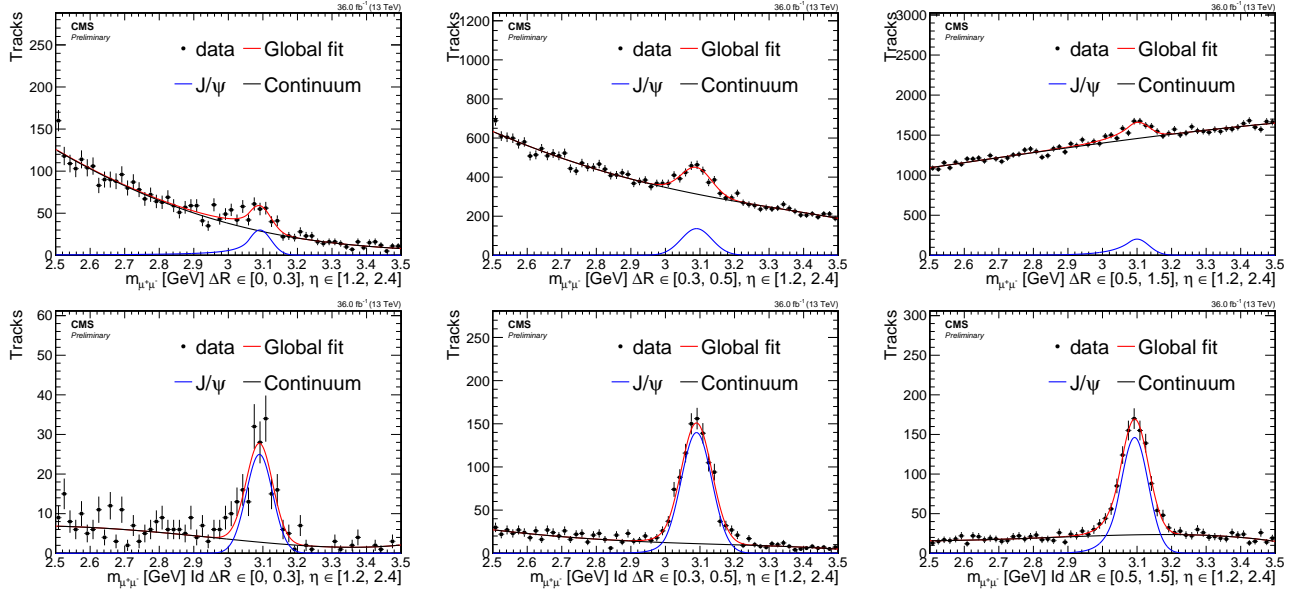
Figure 6.18: Endcaps Muons Data

Chapter 7

Jet Isolation and Non-Isolated Background Estimation

7.1 Jet Isolation

7.1.1 Optimisation

7.2 Non-Isolated Background

Chapter 8

Summary

Chapter 9

Latex stuff

9.1 Some examples

9.1.1 Multiline comment

This is a line in introduction.

9.1.2 Fixme note

This is the introduction to the thesis. **FiXme Note: This is a fixme note FiXme Note: what FiXme Note: WHAT THE HELL** AFTER

9.1.3 Tables

Table 9.1: Table captions are above the table whereas figure captions are below.

Parameter	Value 1	Value 2
s	10.0	20.0
t	20.0	30.0
u	30.0	40.0

9.1.4 Cross References

9.1.4 31 section 9.1.4

9.1.5 Particles

Hello World $\widetilde{\chi}_1^0 \pi \eta_c$ GeV E_T^{miss} hey GeV E_T^{miss} π new one $\widetilde{\chi}_1^0$ $\widetilde{\chi}_1^0$

9.1.6 Citing

[1] SOS analysis

9.1.7 Glossary

Using glossary for compter computer plural form computers upper case first Computer upper case first plural Computers. To use for symbol π

9.1.8   Acronyms

First use of acronym SOS and second SOS. You can reset this and do again Soft-Opposite-Sign (SOS) and second time again SOS. Long version Soft-Opposite-Sign. Full version Soft-Opposite-Sign (SOS). Short version SOS.

List of Corrections

Glossary

computer is a programmable machine that receives input, stores and manipulates data, and provides output in a useful format. 25

ΔR separation. 17

η pseudorapidity. 17

$E_{\mathrm{T}}^{\mathrm{miss}}$ add description. 12–14

$H_{\mathrm{T}}^{\mathrm{miss}}$ add description. 12–14

$m_{\ell\ell}$ invariant mass. 15

neutralino add description. 12, 13

ϕ azimuthal angle measured in radians. 17

π ratio of circumference of circle to its diameter. 25

p_{T} transverse momentum. 13

Acronyms

DM Dark Matter. 12

ISR Initial State Radiation. 13, 14

LSP Lightest SUSY Particle. 12

QCD Quantum Chromodynamics. 13, 14

SM Standard Model. 11–14

SOS Soft-Opposite-Sign. 15–17, 26

SUSY Supersymmetry. 12

WIMP Weakly Interacting Massive Particle. 12

Bibliography

[1] **CMS** Collaboration, A. Tumasyan *et al.*, "Search for supersymmetry in final states with two or three soft leptons and missing transverse momentum in proton-proton collisions at $\sqrt{s} = 13$ TeV," *JHEP* **04** (2022) 091, arXiv:2111.06296 [hep-ex].

List of Figures

List of Tables